

# Fabrication of High-Performance InGaAsN Ridge Waveguide Lasers With Pulsed Anodic Oxidation

C. Y. Liu, S. F. Yoon, S. Z. Wang, W. J. Fan, Y. Qu, and S. Yuan

**Abstract**—We have demonstrated high-performance InGaAsN triple-quantum-well ridge waveguide (RWG) lasers fabricated using pulsed anodic oxidation. The lowest threshold current density of  $675 \text{ A/cm}^2$  was obtained from a P-side-down bonded InGaAsN laser, with cavity length of  $1600 \mu\text{m}$  and contact ridge width of  $10 \mu\text{m}$ . The emission wavelength is  $1295.1 \text{ nm}$ . The transparency current density from a batch of unbonded InGaAsN RWG lasers was  $397 \text{ A/cm}^2$  (equivalent to  $132 \text{ A/cm}^2$  per well). High characteristic temperature of  $138 \text{ K}$  was also achieved from the bonded  $10 \times 1600\text{-}\mu\text{m}^2$  InGaAsN laser.

**Index Terms**—InGaAsN, laser diode, pulsed anodic oxidation (PAO), ridge waveguide (RWG).

## I. INTRODUCTION

RECENTLY, there has been considerable interest in InGaAsN quantum wells (QWs) grown on GaAs substrate, which is a promising alternative to conventional InP-based technology, for realizing low-cost, high-performance, and high-temperature laser diodes in the  $1.3\text{-}\mu\text{m}$  wavelength regime [1]–[8]. High-performance InGaAsN lasers have been fabricated from structures grown by molecular beam epitaxy (MBE) [1]–[6] and metal-organic chemical vapor deposition (MOCVD) [7], [8]. For MBE-grown InGaAsN lasers in the  $1.3\text{-}\mu\text{m}$  wavelength region, low threshold current density ( $J_{\text{th}}$ ) of  $546 \text{ A/cm}^2$  at room temperature (RT) [1], high continuous-wave (CW) output power of  $8 \text{ W}$  at  $10^\circ\text{C}$  [2] and high characteristic temperature ( $T_0$ ) of  $122 \text{ K}$  [3] have been reported. For MOCVD-grown InGaAsN lasers in the  $1.3\text{-}\mu\text{m}$  wavelength region, Sato *et al.* [7] have reported the highest  $T_0$  of  $205 \text{ K}$  and Tansu *et al.* [8] have reported the lowest  $J_{\text{th}}$  of  $210 \text{ A/cm}^2$ . With regards to InGaAsN edge-emitting lasers, so far most results have been focused on broad area (BA) lasers, while there have been relatively few reports on high-performance InGaAsN ridge waveguide (RWG) lasers [4]–[6], whose application has been practical due to their better electrical and optical confinement properties.

In fabricating laser diodes, a uniform and high-quality current blocking layer is of crucial importance. This layer is conventionally formed by depositing  $\text{SiO}_2$  or  $\text{Si}_3\text{N}_4$  using plasma-enhanced chemical vapor deposition (PECVD). Dallesasse [9]

has applied wet thermal oxidation in the fabrication of AlGaAs lasers for the first time. However, the oxidation process is carried out at a typically high temperature of  $\sim 400^\circ\text{C}$ . Furthermore, this method was limited to high Al content, and the oxidation rate of  $\text{Al}_x\text{Ga}_{1-x}\text{As}$  is highly dependent on the Al composition. Pulsed anodic oxidation (PAO) has been proposed and investigated [10]–[12] to produce high-quality native oxide on compound semiconductor for laser diode fabrication. Compared to PECVD and wet thermal oxidation, the advantage of PAO lies in its low cost, RT, and self-aligned processing nature. Furthermore, photoresist can be used as the mask during oxidation. Therefore, RWGs defined by wet chemical etching and subsequent PAO involves only one photolithography step. In this letter, we report the fabrication of high-performance strain-compensated InGaAsN triple QW (TQW) RWG lasers in the  $1.3\text{-}\mu\text{m}$  wavelength regime using PAO for the first time.

## II. EXPERIMENTAL DETAILS

InGaAsN–GaAs–GaAsP TQW laser structures used in this work were grown by MOCVD. The active region consists of three  $\text{In}_{0.35}\text{Ga}_{0.65}\text{As}_{0.985}\text{N}_{0.015}$  ( $6.4 \text{ nm}$ )/GaAs ( $7 \text{ nm}$ )/ $\text{GaAs}_{0.82}\text{P}_{0.18}$  ( $8 \text{ nm}$ ) QWs, which are embedded in two  $12\text{-nm}$ -thick  $\text{GaAs}_{0.82}\text{P}_{0.18}$  tensile-strained barrier layers. The active region is then symmetrically sandwiched between two  $35\text{-nm}$ -thick undoped GaAs waveguide layers. A  $1.2\text{-}\mu\text{m}$ -thick Si-doped ( $6.4 \times 10^{17} \text{ cm}^{-3}$ ) n-type  $\text{Al}_{0.5}\text{Ga}_{0.5}\text{As}$  lower cladding layer was grown on the  $200\text{-nm}$ -thick  $\text{n}^+\text{-GaAs}$  buffer layer, which was grown on the n-GaAs substrate. A  $1.2\text{-}\mu\text{m}$ -thick C-doped ( $5 \times 10^{17} \text{ cm}^{-3}$ ) p-type  $\text{Al}_{0.5}\text{Ga}_{0.5}\text{As}$  upper cladding layer was grown above the active region, and followed by a  $200\text{-nm}$ -thick  $\text{P}^+$  ( $1.4 \times 10^{19} \text{ cm}^{-3}$ ) GaAs cap layer. Following the standard photolithography process, wet chemical etching was carried out using  $\text{H}_3\text{PO}_4:\text{H}_2\text{O}_2:\text{H}_2\text{O}$  ( $1:1:5$ , by volume) to form the ridge. Photoresist was used as a mask during the etching. The ridge height was  $\sim 1.23 \mu\text{m}$ , for both contact ridge widths of  $4$  and  $10 \mu\text{m}$ , respectively. With photoresist still present on top of the ridge, a  $\sim 200\text{-nm}$ -thick oxide layer was formed using PAO. The experimental setup for PAO was previously reported in [11]. After oxidation and photoresist removal, P-type ohmic contact layers (Ti–Au,  $50/250 \text{ nm}$ ) were deposited by electron beam evaporation. The substrates were then lapped down to  $\sim 100 \mu\text{m}$ . N-type ohmic contact layers (AuGe–Ni–Au,  $150/30/150 \text{ nm}$ ) were deposited on the backside of the substrates. The samples were alloyed at  $410^\circ\text{C}$  for  $3 \text{ min}$  in  $\text{N}_2$  ambient. Individual InGaAsN RWG lasers were then cleaved at different cavity lengths for measurement of laser output power versus injection current ( $P$ – $I$ ) characteristics under CW operation without facet coating.

Manuscript received May 4, 2004; revised June 29, 2004.

C. Y. Liu, S. F. Yoon, S. Z. Wang, and W. J. Fan are with the School of Electrical and Electronic Engineering, Nanyang Technological University, Singapore 639798, Singapore (e-mail: liucy@ntu.edu.sg; esfyoon@ntu.edu.sg; eszwang@ntu.edu.sg; ewjfan@ntu.edu.sg).

Y. Qu and S. Yuan are with the School of Materials Engineering, Nanyang Technological University, Singapore 639798, Singapore (e-mail: yqu@ntu.edu.sg; assyuan@ntu.edu.sg).

Digital Object Identifier 10.1109/LPT.2004.835214

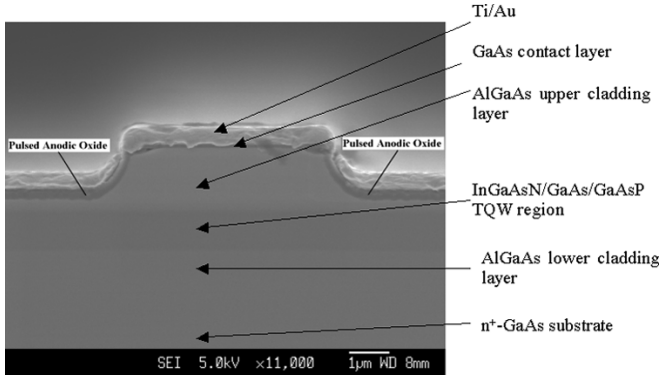


Fig. 1. Cross-sectional SEM image of an InGaAsN RWG laser diode fabricated using PAO, with indicated respective layer structure.

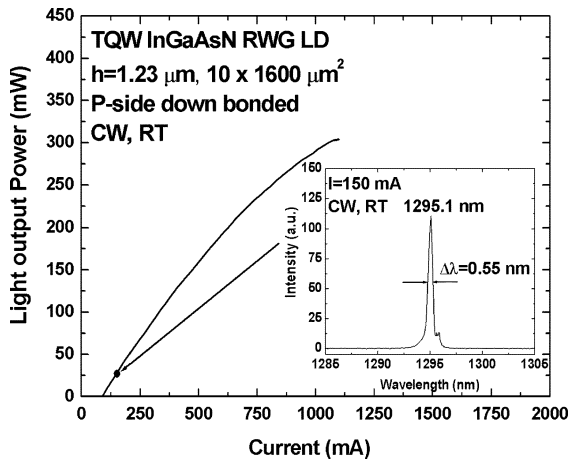


Fig. 2.  $P$ - $I$  characteristic of a bonded  $10 \times 1600$ - $\mu\text{m}^2$  InGaAsN laser diode with  $1.23$ - $\mu\text{m}$  ridge height. Inset shows the emission spectrum of the laser at injection current of  $150$  mA.

### III. RESULTS AND DISCUSSION

Fig. 1 shows a scanning electron microscope (SEM) cross-sectional image of an InGaAsN RWG laser fabricated using PAO, with indicated respective layer structure. For observation convenience, the chosen device has a ridge width of  $4 \mu\text{m}$  for favorable aspect ratio. The dark region seen in Fig. 1 is the oxidized AlGaAs layer above the active region with thickness of  $\sim 200$  nm. No obvious undercutting of the GaAs cap layer was observed in the oxidation process. This is an important aspect for contact metal coverage.

Fig. 2 shows the  $P$ - $I$  characteristics of the InGaAsN TQW RWG laser, with contact ridge width of  $10 \mu\text{m}$  and cavity length of  $1600 \mu\text{m}$  ( $10 \times 1600 \mu\text{m}^2$ ), under CW RT operation. The laser was P-side-down bonded onto a copper heat sink with indium. The laser exhibits threshold current  $I_{\text{th}}$  of  $108$  mA, corresponding to  $J_{\text{th}}$  of  $675 \text{ A/cm}^2$ . The inset shows the emission spectrum of the same laser at injection current of  $150$  mA. A primary mode centered at  $1295.1$  nm was observed.

Fig. 3(a) shows the relationship between the reciprocal of external quantum efficiency ( $\eta_d$ ) and cavity length ( $L$ ) measured from a batch of unbonded InGaAsN TQW RWG lasers with contact ridge width of  $10 \mu\text{m}$ . The cavity length ranges from

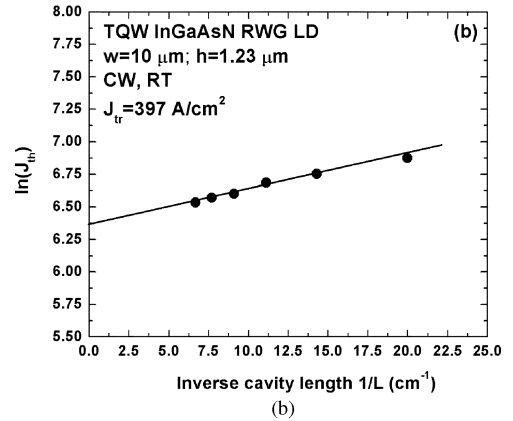
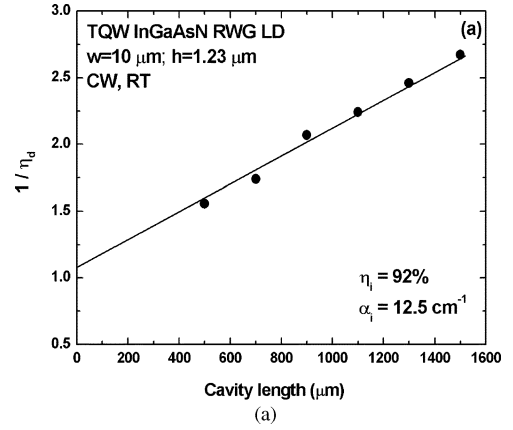


Fig. 3. (a) Plot of inverse external quantum efficiency ( $1/\eta_d$ ) as function of laser cavity length ( $L$ ). The internal quantum efficiency ( $\eta_i$ ) and internal optical loss ( $\alpha_i$ ) were determined to be  $92\%$  and  $12.5 \text{ cm}^{-1}$ , respectively. (b) Plot of threshold current density,  $\ln(J_{\text{th}})$  as function of inverse laser cavity length ( $1/L$ ). The transparency current density ( $J_{\text{tr}}$ ) was determined to be  $397 \text{ A/cm}^2$ .

$500$  to  $1500 \mu\text{m}$ . The internal quantum efficiency ( $\eta_i$ ) and internal optical loss coefficient ( $\alpha_i$ ) were determined to be  $92\%$  and  $12.5 \text{ cm}^{-1}$ , respectively.  $\ln(J_{\text{th}})$  as a function of inverse cavity length ( $1/L$ ) from the same batch of InGaAsN lasers was plotted in Fig. 3(b). The transparency current density ( $J_{\text{tr}}$ ) of the lasers was derived to be  $397 \text{ A/cm}^2$  (equivalent to  $132 \text{ A/cm}^2$  per well) from Fig. 3(b) using the following [13]:

$$\ln J_{\text{th}} = \ln \left( \frac{J_0}{\eta_i} \right) + \frac{\alpha_i}{\Gamma g_0} + \frac{L_{\text{opt}}}{L} - 1 \quad (1)$$

where  $\alpha_i$ ,  $\eta_i$ ,  $\Gamma$ ,  $g_0$  are the internal optical loss, internal quantum efficiency, optical confinement factor, and material gain, respectively. The optimum cavity length is defined as  $L_{\text{opt}} = (1/2\Gamma g_0) \ln(1/R_1 R_2)$ , and  $J_0 = eJ_{\text{tr}}$ .  $R_1 = R_2 = 0.32$  are the optical power reflection coefficients at both facets.

The temperature-dependent  $P$ - $I$  characteristics of a P-side-down bonded  $10 \times 1600$ - $\mu\text{m}^2$  InGaAsN RWG laser are shown in Fig. 4. The inset shows the logarithm of the threshold current  $\ln(I_{\text{th}})$  as function of heat sink temperature in the range of  $20$  °C– $100$  °C.  $T_o$  was estimated to be  $138$  K using the following:

$$I_{\text{th}} = I_o \exp \left( \frac{T}{T_o} \right). \quad (2)$$

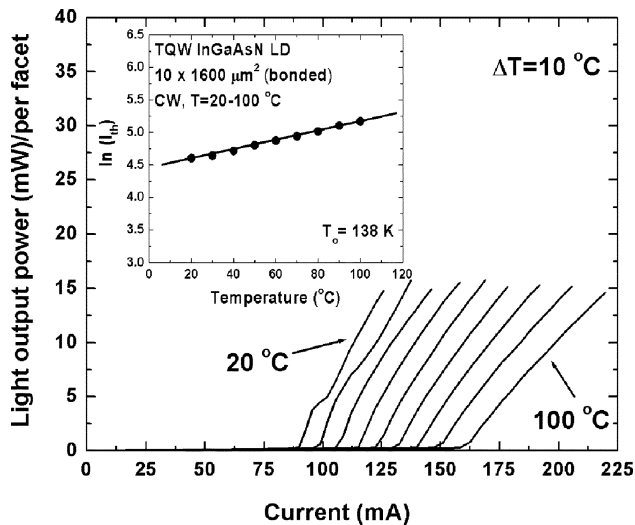


Fig. 4. Temperature-dependent (20 °C–100 °C)  $P$ – $I$  characteristics of a junction-down bonded  $10 \times 1600\text{-}\mu\text{m}^2$  RWG InGaAsN laser. Inset shows a plot of  $\ln(I_{th})$  as function of temperature. The characteristic temperature  $T_0$  was determined to be 138 K.

In a QW laser, comparison of  $J_{th}$  and  $T_0$  is important, as these parameters are typically of practical interest for such devices. Here, we compare the  $J_{th}$  and  $T_0$  of our devices with similar works, and devices fabricated using conventional method on the same wafer as ours. Borchert *et al.* [4] have reported pulsed operation of an InGaAsN RWG [ $3.5 \times 350\mu\text{m}^2$ , double QW (DQW)] laser emitting at  $1.29\mu\text{m}$  with  $J_{th}$  of  $1.31\text{ kA/cm}^2$  and CW operation of an InGaAsN RWG ( $4 \times 700\mu\text{m}^2$ , DQW) laser with  $T_0$  of 110 K. Fischer *et al.* [5] have reported CW operation of an InGaAsN RWG ( $4 \times 600\mu\text{m}^2$ , SQW) laser emitting at  $1.29\mu\text{m}$  with  $J_{th}$  of  $875\text{ A/cm}^2$  and  $T_0$  of 160 K, while Ha *et al.* [6] have reported pulsed operation of an InGaAsN RWG ( $20 \times 770\mu\text{m}^2$ , TQW) laser emitting at  $1.315\mu\text{m}$  with  $J_{th}$  of  $1.31\text{ kA/cm}^2$  and  $T_0$  of  $\sim 65\text{ K}$ .

Using the same wafer as ours as presented in this work, InGaAsN RWG lasers with contact ridge width of  $2\mu\text{m}$  and BA lasers with contact ridge width of  $50\mu\text{m}$  were fabricated with conventional  $\text{SiO}_2$  confinement deposited by PECVD [14], [15]. For a P-side-up bonded uncoated  $2 \times 400\text{-}\mu\text{m}^2$   $\text{SiO}_2$ -confined RWG InGaAsN laser,  $J_{th}$  of  $\sim 1.875\text{ kA/cm}^2$  at RT, and  $T_0$  of 135 K were obtained [14]. For a  $50 \times 1200\text{-}\mu\text{m}^2$   $\text{SiO}_2$ -confined BA laser,  $J_{th}$  of  $\sim 1.1\text{ kA/cm}^2$  was obtained [15]. Compared with the above-mentioned published data [4]–[6], and results from devices fabricated using conventional  $\text{SiO}_2$  confinement on the same wafer as ours [14], [15], we have shown that InGaAsN TQW RWG lasers fabricated using the simple PAO technique showed better, or comparable performance with the lowest  $J_{th}$  of  $675\text{ A/cm}^2$ ,  $J_{tr}$  of  $397\text{ A/cm}^2$  (equivalent to  $132\text{ A/cm}^2$  per well), and high  $T_0$  of 138 K. Overall, in terms of  $J_{th}$  and  $T_0$ , these results are among the best for InGaAsN RWG lasers in the  $1.29 \sim 1.30\mu\text{m}$  wavelength regime ever reported.

It can be seen that devices fabricated using the PAO process exhibit high performance. Since the native oxide was formed by consuming a part of the semiconductor material, better passivation of the sidewalls after wet etching can be expected. Fur-

thermore, the laser fabrication process with PAO is much simpler than that of conventional method using  $\text{SiO}_2$  confinement, which could have also contributed to the high performance of the device by minimizing the possibility of process variations.

#### IV. CONCLUSION

High-performance InGaAsN strain-compensated TQW RWG lasers have been fabricated using the PAO technique, which is relatively simple, cost-effective, and reliable. The lowest  $J_{th}$  of  $675\text{ A/cm}^2$  was obtained from a P-side-down bonded as-cleaved  $10 \times 1600\text{-}\mu\text{m}^2$  InGaAsN laser with emission wavelength of  $1295.1\text{ nm}$ . The  $J_{tr}$  from a batch of unbonded as-cleaved InGaAsN RWG lasers was  $397\text{ A/cm}^2$  (equivalent to  $132\text{ A/cm}^2$  per well). The P-side-down bonded  $10 \times 1600\text{-}\mu\text{m}^2$  InGaAsN RWG laser also exhibited high  $T_0$  of 138 K.

#### REFERENCES

- [1] W. Li, T. Jouhti, C. S. Peng, J. Kontinen, P. Iaukkanen, E.-M. Pavlescu, M. Dumitrescu, and M. Pessa, "Low-threshold-current  $1.32\text{-}\mu\text{m}$  GaInNAs/GaAs single quantum-well lasers grown by molecular-beam epitaxy," *Appl. Phys. Lett.*, vol. 79, no. 21, pp. 3386–3388, Nov. 2001.
- [2] D. A. Livshits, A. Y. Egorov, and H. Riechert, "8 W continuous wave operation of InGaAsN lasers at  $1.3\mu\text{m}$ ," *Electron. Lett.*, vol. 36, no. 16, pp. 1381–1382, Aug. 2000.
- [3] J. Wei, F. Xia, C. Li, and S. R. Forrest, "High  $T_0$  long-wavelength InGaAsN quantum-well lasers grown by GSMBE using a solid arsenic source," *IEEE Photon. Technol. Lett.*, vol. 14, pp. 597–599, May 2002.
- [4] B. Borchert, A. Y. Egorov, S. Illek, and H. Riechert, "Static and dynamic characteristics of  $1.29\text{-}\mu\text{m}$  GaInNAs's ridge-waveguide laser diodes," *IEEE Photon. Technol. Lett.*, vol. 12, pp. 597–599, June 2000.
- [5] M. Fischer, D. Gollub, M. Reinhardt, and M. Kamp, "GaInNAs's for GaAs based lasers for the  $1.3$  to  $1.5\mu\text{m}$  range," *J. Cryst. Growth*, vol. 251, no. 1–4, pp. 353–359, Apr. 2003.
- [6] W. Ha, V. Gambin, M. Wistey, S. Bank, S. Kim, and J. S. Harris Jr., "Multiple quantum well GaInNAs-GaNAs's ridge-waveguide laser diodes operating out to  $1.4\mu\text{m}$ ," *IEEE Photon. Technol. Lett.*, vol. 14, pp. 591–593, May 2002.
- [7] S. Sato, "Low threshold and high characteristics temperature  $1.3\mu\text{m}$  range GaInNAs's lasers grown by metalorganic chemical vapor deposition," *Jpn. J. Appl. Phys.*, vol. 39, pp. 3403–3405, June 2000.
- [8] N. Tansu, J.-Y. Yeh, and L. J. Mawst, "High-performance  $1200\text{-nm}$  InGaAs and  $1300\text{-nm}$  InGaAsN quantum-well lasers by metalorganic chemical vapor deposition," *IEEE J. Select. Topics Quantum Electron.*, vol. 9, pp. 1220–1227, Sept./Oct. 2003.
- [9] J. M. Dallesasse and N. Holonyak Jr., "Native-oxide stripe-geometry  $\text{Al}_x\text{Ga}_{1-x}\text{As-GaAs}$  quantum well heterostructure lasers," *Appl. Phys. Lett.*, vol. 58, no. 4, pp. 394–396, Jan. 1991.
- [10] M. J. Grove, D. A. Hudson, P. S. Zory, R. J. Dalby, C. M. Harding, and A. Rosenberg, "Pulsed anodic oxides for III-V semiconductor device fabrication," *J. Appl. Phys.*, vol. 76, no. 1, pp. 587–589, July 1994.
- [11] S. Yuan, C. Jagadish, Y. Kim, Y. Chang, H. H. Tan, R. M. Cohen, M. Petravic, L. V. Dao, M. Gal, M. C. Y. Chan, E. H. Li, S. O. Jeong, and P. S. Zory Jr., "Anodic oxide induced intermixing in GaAs/AlGaAs quantum well and quantum wire structures," *IEEE J. Select. Topics Quantum Electron.*, vol. 4, pp. 629–635, July/Aug. 1998.
- [12] C. Y. Liu, S. Yuan, J. R. Dong, S. J. Chua, M. C. Y. Chan, and S. Z. Wang, "Temperature-dependent photoluminescence of GaInP/AlGaInP multiple quantum well laser structure grown by metalorganic chemical vapor deposition with tertiarybutylarsine and tertiarybutylphosphine," *J. Appl. Phys.*, vol. 94, no. 5, pp. 2962–2967, Sept. 2003.
- [13] S. L. Chuang, *Physics of Optoelectronic Devices*. New York: Wiley, 1995.
- [14] S. Yuan, C. Y. Liu, and Y. Qu, "Device Characterization Report on Dilute Nitride RWG Lasers," School Materials Engineering, Nanyang Technological Univ.
- [15] P. Modh and A. Larsson, "Report on Characterization of InGaAsN Laser Material," Chalmers Univ. Technology, Sweden.